BioSystems 208 (2021) 104502

Contents lists available at ScienceDirect

BioSystems

journal homepage: www.elsevier.com/locate/biosystems

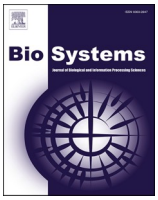

Spatial waves and temporal oscillations in vertebrate limb development

Stuart A. Newman [a,*], Ramray Bhat [b], Tilmann Glimm [c]

[a] Department of Cell Biology and Anatomy, New York Medical College, Valhalla, NY, 10595, USA
[b] Department of Molecular Reproduction, Development and Genetics, Biological Sciences Division, Indian Institute of Science, Bangalore, 560012, India
[c] Department of Mathematics, Western Washington University Bellingham, WA, 98229, USA

ARTICLE INFO

Keywords:
Limb skeletogenesis
Morphogenetic field
Lyapunov function
Reaction-diffusion
Galectin

ABSTRACT

The mesenchymal tissue of the developing vertebrate limb bud is an excitable medium that sustains both spatial and temporal periodic phenomena. The first of these is the outcome of general Turing-type reaction-diffusion dynamics that generate spatial standing waves of cell condensations. These condensations are transformed into the nodules and rods of the cartilaginous, and eventually (in most species) the bony, endoskeleton. In the second, temporal periodicity results from intracellular regulatory dynamics that generate oscillations in the expression of one or more gene whose products modulate the spatial patterning system. Here we review experimental evidence from the chicken embryo, interpreted by a set of mathematical and computational models, that the spatial wave-forming system is based on two glycan-binding proteins, galectin-1A and galectin-8 in interaction with each other and the cells that produce them, and that the temporal oscillation occurs in the expression of the transcriptional coregulator Hes1. The multicellular synchronization of the Hes1 oscillation across the limb bud serves to coordinate the biochemical states of the mesenchymal cells globally, thereby refining and sharpening the spatial pattern. Significantly, the wave-forming reaction-diffusion-based mechanism itself, unlike most Turing-type systems, does not contain an oscillatory core, and may have evolved to this condition as it came to incorporate the cell-matrix adhesion module that enabled its pattern-forming capability.

1. Introduction: spatial and temporal waves in animal development

The bodies of most animal phyla exhibit spatially periodic structures, which is obvious in segmented forms like arthropods, annelid worms, and vertebrates. These examples show that segmentation is widely dispersed in the metazoans and has multiple origins, since these groups do not derive from a common segmented ancestor. Spatial periodicity is also seen in phyla lacking segmented bodies as adults: the tentacles of cnidarian hydra and molluscan octopuses are evenly spaced around the respective mouth regions, and the appendages of echinoderm starfish, often five in number but up to several dozen depending on the species, are uniformly distributed around the central organ-containing region. Furthermore, spatially repetitive ectodermal appendages such as feathers and hairs are commonly seen in birds and mammals. This suggests that the generation of regularly repeated structures is an inherent property of developing animal tissues.

When the tissue properties and processes responsible for such repeated structures have been investigated, they nearly always are found to be based on one of two processes: temporal oscillations in gene expression, or reaction-diffusion systems, with "reaction" and "diffusion" understood broadly to contain multiplicities of biosynthetic production and extracellular transport processes (although segmentation in long germband insects appears to provide an exception; see below). The latter systems, which are often termed "Turing-type" mechanisms in recognition A.M. Turing's early work on the mathematics of such processes, can produce standing waves of chemical concentration or cell density (Kondo and Miura, 2010; Turing, 1952).

An example of an oscillation-based patterning system, the "clock and wavefront" mechanism (a formal version of which was originally proposed nearly 50 years ago (Cooke and Zeeman, 1976)), holds that cells of the presegmental plate of the central body axis of vertebrate embryos, on either side of the neural tube, express gene regulatory proteins (always including one or more of those of the Hairy/Enhancer of Split (Hes) family) in a temporally periodic fashion (Hubaud and Pourquie, 2014). As the embryo elongates, portions of tissue become sufficiently distant from an inhibitory determination front emanating from the embryo's tail tip and organize into paired tissue blocks – *somites*. Each successively forming somite becomes individuated from the unsegmented plate all at once, so their cells must be in the same responsive state just as they

* Corresponding author.
E-mail address: newman@nymc.edu (S.A. Newman).

https://doi.org/10.1016/j.biosystems.2021.104502
Received 11 April 2021; Received in revised form 3 August 2021; Accepted 3 August 2021
Available online 5 August 2021

receive the determination signal. The responsive state of the disinhibited tissue is associated with a specific phase of the Hes cycle. For the cohort of cells defining a forming somite to react in concert, then, they need to be synchronous with respect to the oscillation (Özbudak and Lewis, 2008). The segmenting embryo does not require a special mechanism to achieve such synchrony, however. It occurs in the cells of the segmental plate as in other living (e.g., flashing fireflies) and nonliving (e.g., metronomes on a flexible board) systems spontaneously, owing to weak, nonspecific interactions (Garcia-Ojalvo et al., 2004; Strogatz, 2003).

While the clock-and-wavefront model is generally accepted, not all vertebrate species fully conform to this paradigm, and alternative mechanisms have been proposed for some of them (Stern and Piatkowska, 2015). One of these (also originally due to (Cooke and Zeeman, 1976)) employs a locally self-organizing system in which each forming somite helps induce the one behind it (Cotterell et al., 2015). Like the clock and wavefront model, this reaction-diffusion-based mechanism depends on the oscillatory expression of one of the Hes family proteins and products of other regulatory genes. Interestingly, when parameters are set to values outside their normal ranges, the system can lead to simultaneous, rather than progressive, formation of somites by a spatial standing wave-generating process characteristic (as mentioned) of Turing-type systems.

The deep connection between temporal and (most) spatial wave-forming systems can be obscured in the tissues of developing embryos because of the complex, multiscale nature of these materials. But simpler chemical systems or abstract mathematical models often display the occurrence of both temporal and spatial waves (Cross and Hohenberg, 1993). For instance, in excitable systems like the Oregonator or the Fitzhugh-Nagumo equations, a Hopf bifurcation which leads key variables to undergo oscillations in time, readily gives rise to an instability producing spatial spiral waves when diffusion of system components introduces a spatial dimension into the dynamics (Jahnke et al., 1988). The co-occurrence of Hopf bifurcations and Turing bifurcations (Hopf-Turing bifurcations) capable of generating standing waves is another well-known phenomenon (Just et al., 2001).

As noted, somitogenesis involves synchronization of oscillations in the expression of Hes1. Synchronization occurs within tissue blocks on either side of the neural tube, causing prospective somites to respond to morphogenetic signals, i.e., those that induce regionalization or local cell rearrangement, in a concerted fashion. Since it does not require transport of materials such as morphogens or ions between or through a tissue, synchrony of cellular oscillators is an efficient way to bring about this coordination, since it acts without attenuation over distances greater than molecular diffusion or facilitated transport. It can therefore occur rapidly over tens to hundreds of cells (Chen et al., 2017; Garcia-Ojalvo et al., 2004; Özbudak and Lewis, 2008). Such synchrony can be brought about by entrainment between neighboring subunits that oscillate autonomously (the "Kuramoto effect" (Strogatz, 2003)). Alternatively, it may emerge only when cells interact with one another via juxtacrine-type mechanisms (Hubaud et al., 2017).

Since it is based on an inherently periodic cell function, a synchronized tissue will not necessarily be equally susceptible to developmental factors at all phases of the "clock." This predisposes tissues incorporating a synchronized temporal oscillator to produce repetitive structural modules. In this sense, metamerism as reflected in somites, and in body segments of invertebrates, may originally have been a side-effect of cell synchrony as an adaptive property of developmental systems, given that temporal oscillations are also seen in cell populations such as neural progenitors that do not participate in spatially periodic morphogenesis (Ochi et al., 2020). The metameres could have found adaptive roles after-the-fact, in a "phenotype-first" scenario (West-Eberhard, 2003).

Insect segmentation is another good illustration of patterning processes dependent on oscillations and waves and their possible connections. Developing short germband insects such as beetles and grasshoppers, and other arthropods like centipedes and spiders, employ autonomous intracellular oscillators that organize segments in a spatially progressive fashion in a cellular tissue, utilizing mechanisms that are akin to those that operate in vertebrate embryos (El-Sherif et al., 2012). In contrast, evolutionarily later-appearing long germband insects, such as the fruit-fly *Drosophila* produce their segments by an entirely different, non-oscillator-based mechanism. In these organisms, a syncytial embryo (i.e., all nuclei at this stage residing in a common cytoplasm) in which transcription factors and their mRNAs can diffuse between nuclei, generate regularly spaced stripes of some of the factors using (in some cases) specific stripe-dedicated promoters which are activated or inhibited by spatially dependent concentrations of non-periodically distributed "prepatterning" factors (Clark et al., 2019).

The close phylogenetic relationships among the species exhibiting these disparate segmentation mechanisms have led to the proposal that they are variations on the same process: specifically, it was suggested that the derived long germband mechanism arose from a Turing-type process that appeared spontaneously when a short germband cellular oscillator came to function in a syncytium (Newman, 1993; Salazar-Ciudad et al., 2001). The elaborate multi-enhancer machinery is thus hypothesized to be a "genetically reinforced" (via enhancer duplication and diversification) version of a primordial standing-wave generator. The recent identification of an underlying oscillator in long germband segmentation provides support for this speculation (Verd et al., 2018). Moreover, the existence of intermediate germband insects, which exhibit both progressive sequential segmentation in a cellularized portion of the embryo and simultaneous segmentation in a syncytial region suggests that these are variations on the same mechanism (Clark, 2017; Salazar-Ciudad et al., 2001).

2. Spatial periodicities of the vertebrate limb skeleton

The tetrapod limbs – paired appendages of amphibians, reptiles, birds, and mammals – have skeletons that are quasi-periodic, suggesting the operation of an underlying wave-generating mechanism. The periodicity of the limb skeleton is most evident along the anteroposterior axis, which in the hand, for example, is oriented from the thumb to little finger. This repetition is exemplified by the dual parallel elements (radius and ulna; tibia and fibula) within the mid-region of the limb

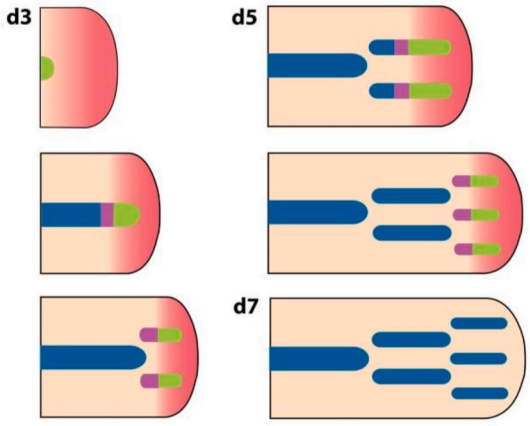

Fig. 1. Schematic representation of development of a vertebrate limb (in this example, the chicken wing between 3 and 7 days of embryogenesis). The proximodistal appearance of the quasi-harmonic series represented by the stylopodium, zeugopodium, and autopodium is shown, with protocondensations shown in green, mature condensations shown in purple, and differentiated cartilage shown in blue. The elements of the zeugopod and autopod, respectively, exhibit periodicity. The rose shading indicates the morphogenetically active zone where synchronization of Hes1 is occurring simultaneously with the organization of the mesenchyme into protocondensations. (See main text for details.)

(zeugopod), and the serially repetitive parallel elements (digits) of the terminal region (autopod) (Hinchliffe and Johnson, 1980) (Fig. 1). There is also a mathematical regularity in the segmental pattern along the proximodistal or long axis of the limb, where successive bones, starting with the humerus or femur (the stylopod), followed by those of the zeugopod and autopod, form a tandem series of elements (Young et al., 2015). Since the lengths of these are different from one another, the allocation of tissue domains in the respective regions do not seem to be by a wave-generating or oscillatory process (Fig. 1) and may instead be determined by competing proximal and distal signals (Roselló-Díez et al., 2014). A striking feature of the organization of the proximodistal axis throughout the tetrapods, even pertaining to the closely related lobe-finned fishes, is the generally arithmetical increase in the number of elements in each successively distal segment.

As we describe below, based on experimental studies on embryonic limbs and limb bud cells in vitro, and associated mathematical and computational models, both a standing wave generator and an oscillator are involved in producing the anteroposterior periodicities. Unlike the respective waves and oscillators of somitogenesis and insect segmentation, however, these are not the same dynamical system in different contexts. Rather, the spatial periodicities (e.g., digits) appear to be generated by a local activation/lateral inhibition-type process, while the outcomes of this pattern-forming system are sharpened and refined by a separate temporal oscillator that interacts with it.

One feature of a standing wave generator that makes it a plausible mechanism for vertebrate limb skeletogenesis is the straightforward way in which a harmonic series of elements can be generated as tissue parameters, including size and shape, but also regulatory factors such as Hox proteins and fibroblast growth factor receptors (FGFRs), change. This has permitted a natural account of the proximodistal increase in number of skeletal elements (Newman and Frisch, 1979; Hentschel et al., 2004; Zhu et al., 2010; Bhat et al., 2016) (see below).

During development, the limb buds of vertebrate species protrude from the body wall, or flank, at four discrete sites – two for the forelimbs and two for the hindlimbs. The mesoblast, a paddle-shaped mass of mesenchymal tissue that gives rise to the skeleton and muscles, is enclosed by a simple epithelial layer, the ectoderm. The skeletons of vertebrate limbs typically develop in a proximal to distal order, that is, the parts destined to be closest to the body form earliest, followed by structures progressively distant from the body (Fig. 1). This occurs initially as a series of cellular condensations in the precartilage mesenchyme; these, in turn, differentiate into cartilage in the same order. Finally, in species with bony limb skeletons (birds and mammals, for example), the cartilaginous elements are replaced by bone. Urodele salamanders provide some exceptions to this proximodistal progression (Franssen et al., 2005).

As with the somites of the primary body axis and the segments of insects, the repetitive elements of the limb are not exact repeats. This means that superimposed on the periodicity generating process is an individuating one that makes the digits in an autopod different from one

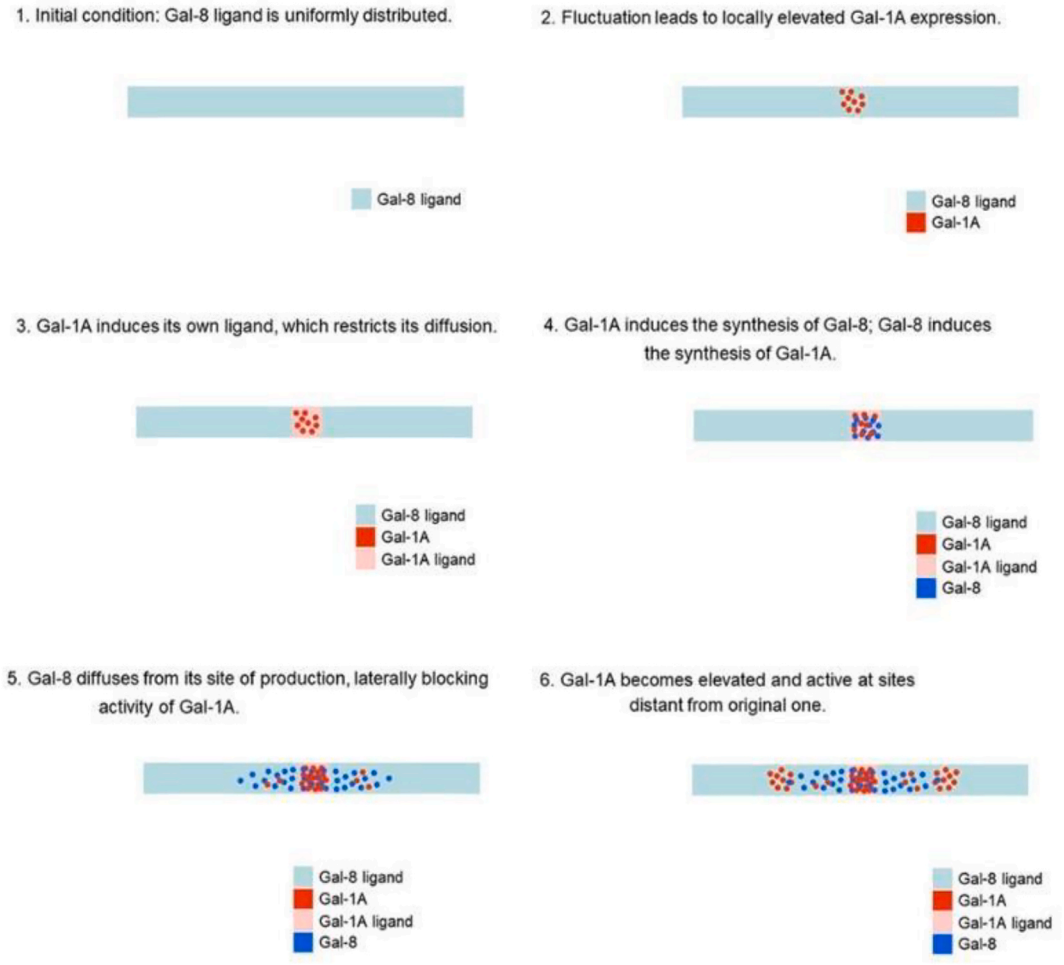

Fig. 2. Qualitative model, based on experiments of (Bhat et al., 2011), for spatial organization of protocondensations by the interactions of galectin counterreceptor-expressing precartilage mesenchymal cells with Gal-1A and Gal-8. (See main text for details.)

another, for example. As with somitogenesis and insect segmentation, this role is partly served by nonuniform, aperiodic distributions of Hox class gene products. The locations and identities of the zeugopodium and digits were long thought to be specified by a common underlying "positional information" system, but evidence now favors a determining role for self-organizing mechanisms, specifically ones based on Turing-type processes, in setting these patterns (Cooper, 2015). In addition to the galectin-based "2GL" mechanism discussed below, Turing-type mechanisms involving transforming growth factor-β, fibroblast growth factor and its receptors, and fibronectin (the TFF model; Hentschel et al., 2004), and bone morphogenetic factor, transcription factor Sox9, and Wnt (the BSW model; Raspopovic et al., 2014) are thought to act in an overlapping fashion at various points in development, apparently having appeared at different times during tetrapod evolution (Newman et al., 2018).

Two additional models, by Badugu et al. (2012) and Lange et al. (2018) demonstrate that Turing-type self-organization can occur even in the absence of diffusible activators and inhibitors (a feature also of the 2GL system, the focus of this paper). The first of these depends on excitable feedback interactions between the production of BMP and its receptor to obviate some of the standard requirements of the Turing system. The model of Lange et al. (2018) has the formal logic of a Turing reaction-diffusion system, but postulates a bistable intrinsic cell state (either "on" or "off" for the cartilage differentiation pathway) that propagates across the tissue by an unspecified mechanism, possibly, but not necessarily diffusion (Lange et al., 2018). The analysis of the 2GL system presented below may, in fact, instantiate the bistable switch hypothesized by Lange and coworkers.

The refutation of positional information as the basis for quasi-periodic skeletal pattern has not disconfirmed the large body of knowledge on determination of the identity of skeletal elements by ancillary molecules, often in a species-specific fashion. In addition to Hox gene products, these include the morphogen Sonic hedgehog, and retinoids and their receptors. Such factors are distributed nonuniformly across the limb bud as the skeletal elements form, causing structures that would otherwise be equivalent to become recognizably different (McQueen and Towers, 2020).

3. The 2GL model: a reaction-diffusion-adhesion mechanism generating repetitive skeletal elements

As mentioned above, the cartilage elements that serve as the primordia of the limb skeleton are prefigured developmentally by mesenchymal condensations. Unlike cartilage itself, which consists of well-spaced cells, i.e., chondrocytes, condensations comprise undifferentiated cells that have been drawn into tight knots within the surrounding loosely packed mesenchyme by the extracellular matrix (ECM) protein fibronectin. Up to a day before overt condensations appear, however, the cells destined to form them undergo a subtler clustering termed "compaction" (Barna and Niswander, 2007) or "protocondensation" (Bhat et al., 2011). The formation of protocondensations requires signaling by the growth factor BMP, and in birds, two proteins, Gal-1A and Gal-8 (Bhat et al., 2011), members of the galectin class of animal lectins with binding affinity to β-galactosides (Kaltner and Gabius, 2012).

Fibronectin is not yet present when protocondensations arise (Bhat et al., 2011), and although the cartilage-associated transcription factor Sox9 has already appeared, it is not required for their formation (Barna and Niswander, 2007). Therefore, standing wave-generating mechanisms like the TGF-β-fibronectin-FGF (TFF) model (Hentschel et al., 2004) and the BMP-Sox9-Wnt (BSW) model (Raspopovic et al., 2014) though well-supported by experimental evidence, do not appear to determine the pattern of the skeletal elements during development (at least in birds). Rather, these processes may be superimposed on the originating one to reinforce or stabilize their outcomes (Newman et al., 2018).

Bhat and coworkers investigated the role of Gal-1A and Gal-8 (alternatively CG (chicken galectin) -1A and −8) in the formation of limb protocondensations in the chicken embryo in ovo, and in high-density ("micromass") cell cultures isolated from the respective limb buds (Bhat et al., 2011). They found that staining for mRNA and protein of both galectins, marking the sites of future condensations, was detectable as early as 9 h of incubation. As development progresses, production of these proteins is enhanced at these sites, increasing dramatically for about 36 h, and then rapidly decreasing. The authors found that Gal-1A and Gal-8 formed a positive feedback loop: adding exogenous Gal-1A caused an increase in Gal-8 expression and vice versa. Yet, exogenously added Gal-1A and Gal-8 were found to have opposite effects on condensations. Adding Gal-1A resulted in an increase in the number of condensations. For high doses of Gal-1A, fusion of condensations was observed. In contrast, adding Gal-8 led to fewer, less defined condensations. In turbidimetric experiments, the authors found that Gal-1A mediates cell-cell adhesion, while Gal-8 impairs the ability of Gal-1A to do so.

The investigators also assayed for the presence and developmental regulation of cell surface binding moieties for the galectins (alternatively termed "ligands" or "counterreceptors"). This involved indirect analysis since the identities of the respective molecules are not known. Within these limitations, the following inferences were made: (1) there could be two types of counterreceptors: a shared one, which both Gal-1A and Gal-8 can bind to, and a specific one to which only Gal-8 can bind (given that Gal-8 is a tandem repeat galectin with two distinct glycan-binding domains, whereas Gal-1A is a prototype galectin with a single glycan binding domain); (2) Gal-1A induces the production of the shared counterreceptor; (3) the Gal-8-exclusive counterreceptor is constitutively produced, independently of galectin condensations.

The findings that the production of Gal-1A is under the positive control of Gal-8, and vice versa, along with those showing that cell-cell adhesion is mediated by Gal-1A and antagonized by Gal-8 and the above inferences about counterreceptor regulation, led to a qualitative picture for how the generation of spatially repetitive protocondensations could form: 1) Initial condition, Gal-8 counterreceptor is uniformly distributed; 2) a fluctuation in the uniform field of precartilage mesenchymal cells leads to elevated Gal-1A at a focal site; 3) increased Gal-1A leads to increased Gal-8; increased Gal-8 leads to increased Gal-1A; 4) increased Gal-1A leads to increased shared counterreceptor, trapping both galectins; 5) some Gal-8 diffuses away and builds up in the adjacent regions because of the availability there of its specific receptor; 6) at a critical distance from the original focus, Gal-8 is sufficiently low for induction of additional auto-enhancing foci (Fig. 2).

Glimm and coworkers devised a mathematical model to determine whether there were plausible biological conditions under which this hypothetical scenario could be realized (Glimm et al., 2014). The two-galectin + ligands (2GL) model consists of a system of three partial differential equations, the variables of which are the cell density and the concentrations of Gal-1A and Gal-8. The (generalized) cell density is a function of the concentrations of free shared counterreceptors l_1, free Gal-8 counterreceptors l_8 and shared counterreceptors bound to Gal-1A or Gal-8, c_1 and c_8^1, respectively, and the complex of Gal-8 bound to its counterreceptor c_8^1. This yields the following model equations for the cell

density $R(t,x,l_1,l_8,c_1,c_8^1,c_8^8)$ and the densities of diffusible Gal-1A and Gal-8, $c_1^u(t,x)$ and $c_8^u(t,x)$, respectively:

$$\frac{\partial R}{\partial t} = D_R\nabla^2 R - \nabla\cdot(R\,K(c_1,R)) - \frac{\partial}{\partial c_1}\left(\alpha\left(c_1^u,l_1,c_1\right)R\right) - \frac{\partial}{\partial c_8^8}\left(\beta_8\left(c_8^u,l_8,c_8^1\right)R\right) - \frac{\partial}{\partial c_8^1}\left(\beta_1\left(c_8^u,l_8,c_8^8\right)R\right)$$
$$-\frac{\partial}{\partial l_1}\left(\left(\gamma(c_1,l_1) - \beta_1\left(c_8^u,l_8,c_8^8\right) - \alpha\left(c_1^u,l_1,c_1\right)\right)R\right) - \frac{\partial}{\partial l_8}\left(\delta(l_8) - \beta_8\left(c_8^u,l_8,c_8^1\right)R\right)$$

$$\frac{\partial c_1^u}{\partial t} = D_1\nabla^2 c_1^u + \nu\int c_8^8\,RdP - \int \alpha RdP - \pi_1 c_1^u$$

$$\frac{\partial c_8^u}{\partial t} = D_8\nabla^2 c_8^u + \mu\int c_1 RdP - \int \beta_1 RdP - \int \beta_8 RdP - \pi_8 c_8^u$$

The integrals are taken over the domain defined by the range of variations of the counterreceptors ("counterreceptor space") with $dP = dl_1dl_8dc_1dc_8^8dc_8^1$ (See Glimm et al. (2014) for details.).

The Gal-1A-dependent cell-cell adhesion strength, a crucial component of the system, was modeled using the adhesion flux approach of Armstrong et al. (2006). In the above equations, the effective cell velocity was given by

$$K(c_1,R) = \alpha_K c_1 \int_{D_{\rho_0}}\int \tilde{c}_1\,\sigma\left(R\left(t,x+r,\tilde{l}_1,\tilde{l}_8,\tilde{c}_1,\tilde{c}_8^1,\tilde{c}_8^8\right)\right)d\tilde{P}\frac{r}{|r|}d^n r$$

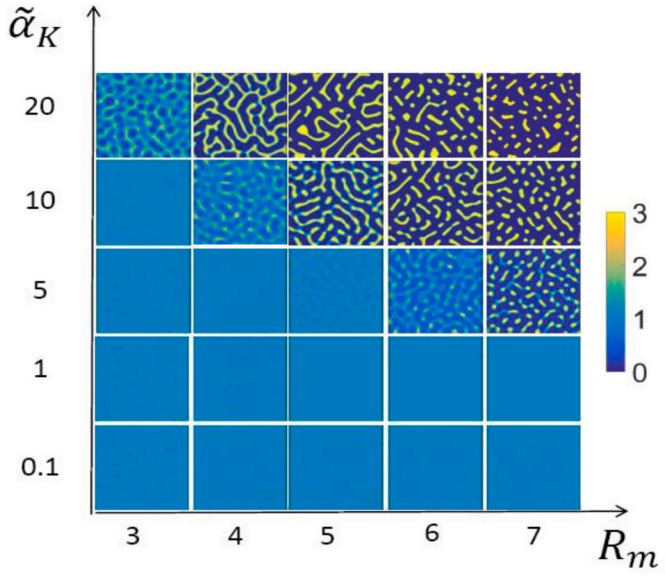

Fig. 3. Cell density patterns in two spatial dimensions produced by the 2GL model. Each small panel shows the final cell density pattern for different values of the parameter $\widetilde{\alpha_K}$, which encodes the strength of cell-cell adhesion mediated by Gal-1A, and R_m , which encodes the maximum cell density, i.e., how densely packed cells within a condensation can be. Similar to simulations in one spatial dimension, below a certain critical curve in the $\widetilde{\alpha_K} - R_m$ diagram no pattern in the cell density can form. Above this curve, an increase of the strength of cell-cell adhesion leads to denser condensations. with sharper boundaries. With the choice of different parameters, the model qualitatively replicates the diversity of possible patterns - labyrinths, stripes and spots - seen in in vitro micromass experiments (Figure from Glimm and Zhang (2020)).

where σ denotes a logistic function and $n = 1, 2$ or 3 is the number of spatial dimensions. Cell-cell adhesion is mediated by c_1, the concentration of the Gal-1A complexed with its counterreceptor. By averaging over the counterreceptor space and over a spatial $n-$ dimensional ball D_{ρ_0} of radius ρ_0, the interaction radius, an effective velocity can be calculated (Armstrong et al., 2006). The 2GL system is only capable of forming periodic arrays of condensations when this adhesion-driven cell movement effect is sufficiently strong (Glimm et al., 2014). This dependence specifies this mechanism as a reaction-diffusion-adhesion (rather than a strictly RD) process.

Simulations in two spatial dimensions showed that for a broad range of parameters, the system can generate regular patterns of high and low cell density, corresponding to sites of condensations with interspersed areas of low cell density (Glimm and Zhang, 2020) (Fig. 3). Moreover, consistent with the experiments of Bhat et al. (2011), increasing the initial Gal-1A concentration in simulations leads to an increase in the number of predicted condensations (peaks in one-dimensional space in this analysis) (Glimm et al., 2014). The effect of increasing Gal-8 was more subtle, and dependent on the percentage of unbound shared receptors, which in turn is determined by the 2GL dynamics. If this percentage was sufficiently low, increasing the initial Gal-8 concentration had the effect (observed in experiments) of reducing the number of peaks of the resulting pattern.

The capacity of the 2GL model to form standing wave patterns is less intuitive than that of classic Turing-type chemically based reaction-diffusion systems, so a qualitative description (a model-informed version of that in Fig. 1) is helpful: the positive feedback loop of the galectin dynamics sets characteristic concentrations of Gal-1A and Gal-8, which in turn determine the adhesion strength between cells. The randomly moving cells react to high concentrations of adhesion-inducing Gal-1A and form clusters (protocondensations) through cell-cell adhesion, leading to spatial patterns in the cell density. These protocondensations tend to be formed by cells with a higher concentration of bound Gal-1A on their membranes than those outside protocondensations because they are 'stickier.' This distinction between cells inside and outside condensations is reinforced as these clusters grow: the density of cells in their environment is depleted, resulting in both a limit to the size of existing clusters and a suppression of the galectin expression positive feedback loop between existent protocondensations. In contrast, the feedback loop is active within protocondensations.

This process falls into the broad category of LALI (local activation, lateral inhibition) mechanisms (Meinhardt and Gierer, 2000). Here, the role of local activation is fulfilled by adhesion-mediated cell-cell aggregation, whereas lateral inhibition, rather than resulting from a diffusible inhibitor, is due to the previously mentioned depletion effect on cell density. The patterning mechanism is *morphodynamic* as opposed to *morphostatic* (in the senses defined by Salazar-Ciudad et al. (2003)): in the case of immobile cells, no chemical prepattern in the galectin concentration can form by the galectin dynamics alone, and thus cell motility is an integral part of the patterning mechanism.

In line with the experimentally motivated schematic in Fig. 2,

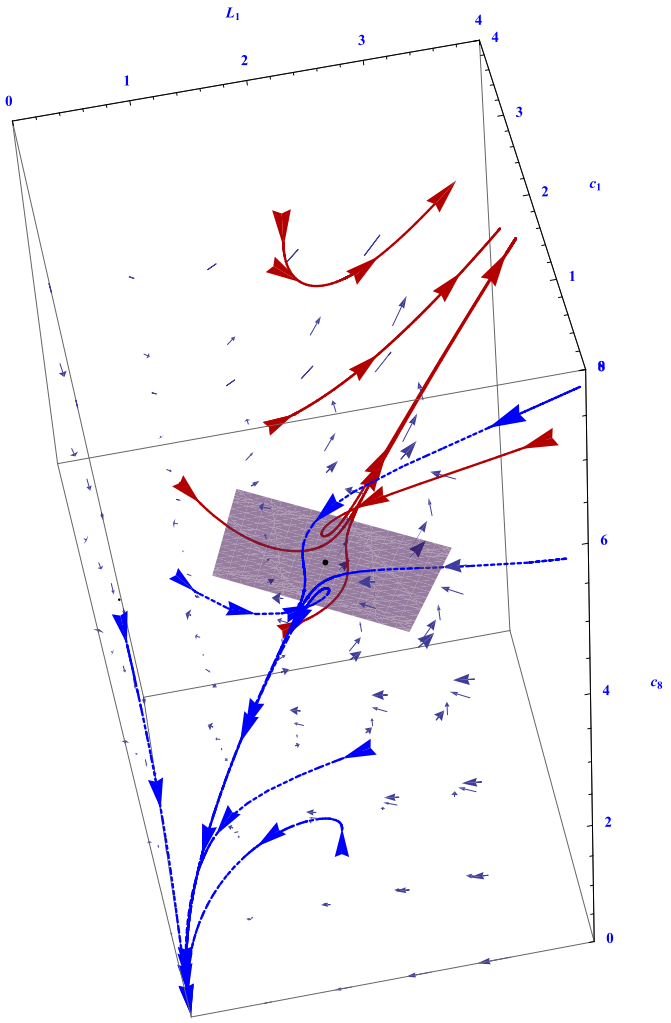

Fig. 4. Phase space of the core switching mechanism of the 2GL network. The axis are concentrations of shared counterreceptors (L_1), Gal-1A (c_1) and Gal-8 (c_8), respectively. Blue dashed trajectories converge to the zero state, corresponding to the 'very low' state of the switch. Red solid trajectories show rapidly increasing concentrations, corresponding to the 'very high' state of the switch. The saddle point is shown with tangent space to the stable manifold, which separates the two dynamic regions. (Parameters $\rho = \sigma = 2,\ \pi = 1.$) (From (Glimm et al., 2021).

however, the spread of Gal-8 provides a mechanism for nonlocal coordination of patterning. The 2GL system can generate structures with varying degrees of periodicity or aperiodicity, a character, along with the wavelength of any periodic patterns, which depends on certain phylogenetic-dependent features of Gal-8 (Bhat et al., 2016).

4. The 2GL system has no temporally oscillating modes

Paired appendages of some extinct vertebrates had arrays of tandemly arranged, regularly spaced skeletal nodules: the ichthyosaur *Brachypterygius*, whose five or six digits each have 8 to 16 similarly sized phalanges is a well-known example (Motani, 1999). This pattern, which echoes repetitive somites, suggests that ancestral versions of the 2GL system may have had intrinsic oscillatory modes in addition to the wave-forming ones described in the previous section. Tetrapods, which do not exhibit such tandemly repetitive motifs, may thus have evolved coordinately with mechanisms that suppressed, intrinsically or extrinsically, temporal oscillations.

One way to approach such possibilities is to analytically isolate the core switching mechanism of the 2GL system to see how it behaves in response to parameter variation independently of its role in spatial patterning. Glimm et al. (2021) derived a system of ordinary differential equations for the reaction arm of the reaction-diffusion-adhesion regulatory network. This can be interpreted as a spatially homogeneous, immobile cell population with fast galectin diffusion. Under the biologically plausible assumption that binding of galectins to counterreceptors happens on a faster time scale than protein production, the core system is given by the equations

$$\frac{dL_1}{dt} = (c_1 - \rho)\, L_1$$

$$\frac{dc_1}{dt} = \frac{1}{\sigma} c_8 - c_1$$

$$\frac{dc_8}{dt} = c_1 L_1 - \pi c_8$$

Here, L_1, c_1 and c_8 are the (nondimensionalized) concentrations of the shared counterreceptor, Gal-1A, and Gal-8, respectively, and ρ, σ, π are parameters of the kinetics. This network exhibits an effectively bistable behavior with the two states corresponding to 'very low' and 'very high' rates of galectin production, respectively. These two states are separated by the stable manifold of a saddle point. (See Fig. 4 for an illustration of this behavior.) The system admits of a Lyapunov function, that is a function which decreases along solution curves, given by

$$\mathscr{L}(L_1, c_1, c_8) = \frac{c_8}{c_1} + \sigma(\pi + 1)\log c_1 - \frac{1}{\rho}c_8 + \frac{1}{\rho}L_1 - \frac{\pi\sigma}{\rho}\log L_1 - \frac{\pi\sigma}{\rho}c_1.$$

The system thus cannot exhibit periodic behavior - the Lyapunov function would have to be constant on such curves, which can be ruled out. Similarly, there are no bounded nonperiodic solutions which do not converge to any equilibrium point, which rules out chaotic behavior. Although damped oscillations with decreasing amplitude are possible close to the saddle point, the characteristic time scale of the decay is so large compared to the period of the oscillations that these oscillations do not have practical relevance, and the core switching mechanism does not exhibit any intrinsic sustained oscillations (Glimm et al., 2021).

5. Oscillation and synchronization of Hes1 gene expression: a role in pattern refinement

A striking feature of protocondensation and condensation formation in high-density cultures derived from chicken limb mesenchyme is the near simultaneity of their formation across the more than 2 mm linear extent of the cultures (Bhat et al., 2019). Cells begin aggregating within a few hours, forming regularly spaced Gal-1A- and Gal-8-rich protocondensations (Bhat et al., 2011). These foci then mature into mature fibronectin-rich condensations (Frenz et al., 1989). Notwithstanding the dispersion in wavelengths and fusion of some adjacent condensations, the emergent patterns robustly reflect the expected outcomes of reaction-diffusion processes (Christley et al., 2007; Glimm et al., 2014; Kiskowski et al., 2004; Raspopovic et al., 2014).

Because Turing-type mechanisms employ diffusion or similarly short-range transport processes, it is difficult for such systems to form reliable patterns over distances much greater than their characteristic wavelengths (e.g., across the developing digital plate or a micromass culture) unless there is very little variation in the initial states of the cells across their domains of action. While this is easy to achieve in theoretical models, such a tight control of initial conditions cannot be assumed *in vivo*. For regular patterning over long distances such systems must incorporate means for effecting global uniformity of cell state. As noted above, synchronization of Hes1 oscillations (via the feedback regulation of juxtacrine Notch and paracrine Wnt signaling) across the width of the presomitic mesoderm constitutes each segmenting band of tissue as a coherently acting cell mass (Aulehla and Pourquie, 2006; Palmeirim et al., 1997). Such regions of developing embryos have been termed "morphogenetic fields" (Gilbert and Sarkar, 2000; Levin, 2012).

While oscillations in the expression of *hes1* (the gene that specifies Hes1) is involved in developmental phenomena other than somitogenesis (in neurogenesis and pancreatic progenitor cell differentiation, for example; (Ochi et al., 2020); (Seymour, 2020)), the 2GL mechanism, as described in Section 3, does not incorporate Hes family gene products, nor is it capable of sustaining temporal oscillations of any of its core components (see Section 4). If long-range patterning of protocondensations is coordinated by cell synchrony, the oscillations do not arise within the basic 2GL system.

However, *hes1* (also known as *c-hairy1* in the chicken) is, in fact, expressed in limb mesenchyme and its overexpression leads to shortening of skeletal elements (Vasiliauskas et al., 2003). As in somitogenesis and other systems, its expression also undergoes periodic changes during limb development. In micromass cultures of limb mesenchyme, Hes1 mRNA concentration oscillated with a period of 6 h, between 12 h and 24 h after plating, the precise time window in which protocondensations appeared. Chemical or surgical manipulation of isolated limb buds, moreover, altered Hes1 localization in a fashion consistent with its oscillatory expression *in vivo* (Bhat et al., 2019).

When *hes1* oscillations were suppressed in micromass cultures by treatment with N- [N- (3,5-difluorophenacetyl-L-alanyl)]-S-phenylglycine *t*-butyl ester (DAPT), an inhibitor of Notch signaling, condensation patterning was perturbed. In early stage micromasses, there was an increase in the number of protocondensations and less regular spacing between them. In mature micromasses, treatment with DAPT brought about a decrease in condensation number, associated with enhanced fusion of neighboring condensations (Fig. 5). The same treatment also markedly increased the expression levels of both Gal-1A and Gal-8 during the formation of protocondensations in vitro (Bhat et al., 2019).

These results raised the possibility of a functional connection between Hes1 oscillations and the core 2GL network. To explore this computationally, we incorporated the effects of oscillatory dynamics on galectin expression in the mathematical model of the 2GL system

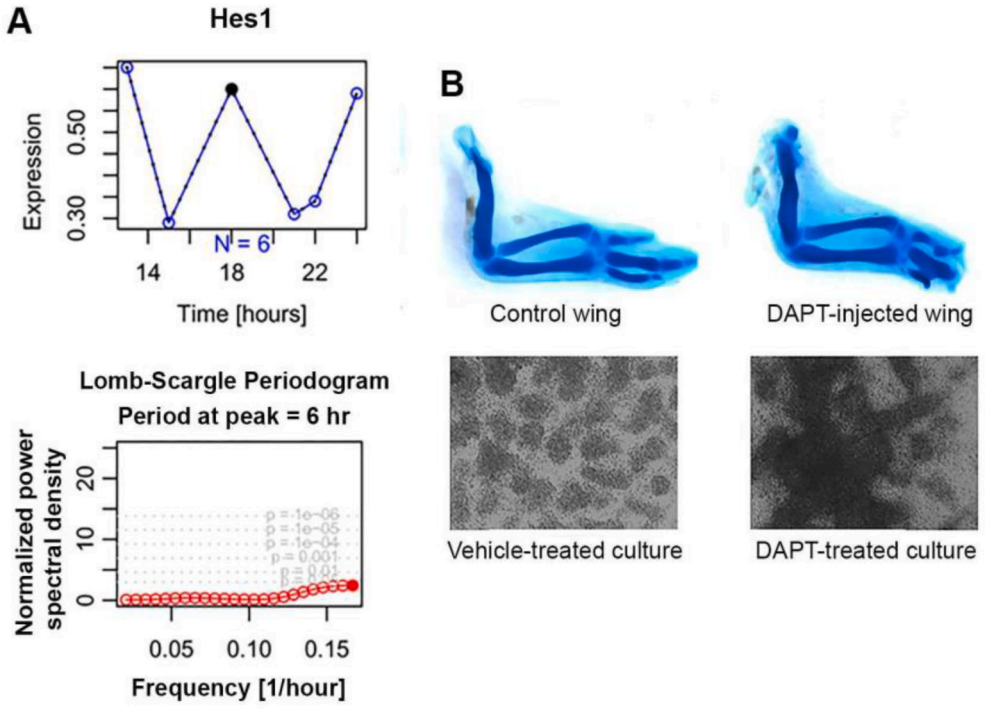

Fig. 5. (A) Analysis of Hes1 mRNA expression (upper panel) by periodograms generated using the Lomb-Scargle algorithm (lower panel). Time intervals of 3, 1, and 0.5 h were used, yielding a consistent periodicity of 6 h. (B) Effects of administering the Hes1 inhibitor DAPT to developing chick limb buds in ovo (upper row) or micromass cultures derived from chick limb bud mesenchymal cells (lower row). In the in ovo experiments, vehicle or vehicle + DAPT was injected into the autopodium about 5½ d of development and the limbs were fixed, stained with Alcian blue, and cleared about 3 d later. In the in vitro experiments, cultures were treated with vehicle or vehicle + DAPT a day after plating and photographed with Hoffman Modulation Contrast optics about 2 days later. In both the in ovo and in vitro cases adjacent precartilage condensations became irregular and underwent fusion, which was reflected in misshapen and fused cartilages in the limb autopod. Figures adapted from Bhat et al. (2019), which can be consulted for details.

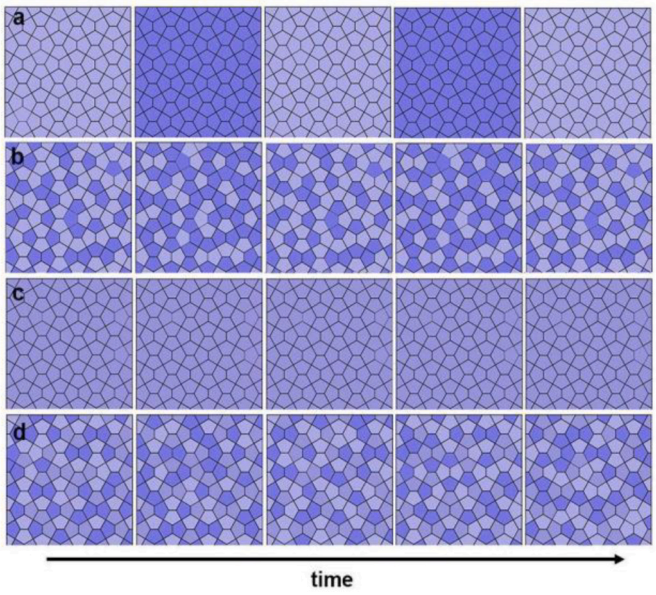

Fig. 6. Schematic representation of change in Hes 1 status in model cells over time, in sets of simulations of the 2GL system modified to include Hes1 phase (Glimm et al., 2021). Rows (a) 'oscillatory synchronous,' (b) 'oscillatory random,' (c) 'nonoscillatory uniform,' (d) 'nonoscillatory random.' While the simulations were performed in 1d, 2d fields of cells corresponding to the micromass culture systems from which experimental data were obtained, are shown. See main text for additional details.

described in Section 3. We introduced an additional function to the model, $\varphi(x,t)$, representing the phase of the Hes1 cycle, and made the adhesion flux (also referred to as haptotaxis) of the cells in response to Gal-1A depend on this phase. This modification was motivated by the clock-and-wavefront mechanism of somitogenesis, where cell rearrangement occurs only during a specific phase range of the Hes1 cycle (Aulehla and Pourquie, 2006; Hubaud and Pourquie, 2014; Palmeirim et al., 1997).

The extended model reproduced, for some galectin diffusion coefficients, the marked rise in both Gal-1A and Gal-8 when Hes1 oscillations were suppressed, justifying its being used to analyze how the presence or absence of Hes1 oscillations, and their synchrony, might affect the character of pattern formation mediated by the 2GL system. We considered alternative scenarios in which (a) oscillations of the Hes1 molecular clock were in phase across the field of cells ('oscillatory synchronous'), (b) the initial phase distribution was random, but cells oscillated with the same frequency ('oscillatory asynchronous'), (c) Hes1 did not oscillate and its expression levels from cell to cell were uniform, i.e., all cells were in the same state ('non-oscillatory uniform'), or (d) Hes1 did not oscillate and its expression levels from cell to cell were random ('non-oscillatory random') (Bhat et al., 2019) (Fig. 6). In each scenario, we averaged over multiple simulations with random non-homogeneous spatial distributions of the initial cell density.

Our (1-dimensional) simulations demonstrated that in both the 'oscillatory synchronous' and 'oscillatory asynchronous' cases, spatial patterns emerged with essentially similar numbers of condensations per unit length. However, patterns that emerged in the synchronous case were markedly more regular than the patterns of the asynchronous counterpart. For non-oscillatory random Hes1 expression, this irregularity was even more pronounced. Whereas in both the synchronous and asynchronous oscillatory cases the irregularity tended to decrease with time through coalescence and re-arrangement of the cell density, this effect was hardly present in the case of non-oscillating random Hes1 expression.

We also performed simulations of the non-oscillatory uniform expression scenario. Here, the Hes1 state was constant in both time and space. The resulting patterns were very similar to the synchronous oscillatory scenario. These comparisons suggested that it is not so much the oscillatory nature of Hes1 expression that is crucial for pattern regularity, but rather the spatial uniformity of the Hes1 state. The significance of synchronization of oscillations may thus be to ensure uniform Hes1 status across the tissue.

Where oscillations of the gene regulatory factor Hes1 are synchronized, as occurs in the presegmental plate mesoderm of vertebrate embryos (Giudicelli et al., 2007; Özbudak and Lewis, 2008) and in the digital plate mesenchyme in ovo and in vitro described here, the levels of this transcriptional co-regulator are rendered identical across a developing primordium at each phase of development. Synchronized oscillations achieve this coordinated state by self-organizational means across long distances relative to the scale of single cells.

6. Conclusions

Oscillations are a frequently observed (and, with certain parameter choices, inevitable) mode of behavior of dynamical systems that contain positive or negative feedback circuits. Moreover, when some of the system's components have different rates of transport across the reaction medium, temporal oscillations can be converted to travelling or standing waves. Since biological systems, in both their intracellular and extracellular aspects, have the requisite properties, temporal and spatial waves can be considered among their "generic" properties. These effects, which can play key roles in organizing periodic patterns and coordinated morphogenetic fields by mechanisms such as those described above, are therefore, from an evolutionary viewpoint, readily acquired, potentially in advance of the functions they will come to serve.

The link between temporal gene expression dynamics and spatial patterning extends across scales in diverse developmental examples. Cyclic expression of Notch signaling controls not just the temporality of somite formation but also the transient expression of *Hoxd1* expression in nascent somites (Rida et al., 2004). Interdisciplinary studies on perturbation of Hox gene functions in transgenic mice show that distally expressed *Hox13* genes regulate digital patterning through controlling the wavelength of a Turing-type self-organizing mechanism (Sheth et al., 2012). It would therefore be worth investigating whether Hox-based regulation intervenes between the effect of Hes1 oscillations (upstream) and the 2GL-based patterning modular activity (downstream) such that the spatially distinct Hox genes tune the galectin reaction-diffusion dynamics to morphologically shape digits in unique ways.

The 2GL model for vertebrate limb pattern formation exhibits a nearly full range of these oscillation- and wave-type phenomena. In the full, spatially dependent, reaction-diffusion-adhesion system, periodic patterns appear that plausibly correspond to the repetitively spaced skeletal elements (cartilage, or dermal bone) in ancestral fish, leading to the periodic arrays of such structures in derived forms including chondrichthyans, actinopterygians, and sarcopterygians. In the latter group, further evolution of Gal-8 at the level of its protein structure, and in the putative *cis*-acting regulators of its gene, appears to have led to the stereotypical quasi-harmonic proximodistal arrangement of the stylopodium, zeugopodium, and autopodium of the tetrapods (Bhat et al., 2016). In the terms of the framework presented here, the generic wave-forming propensity of limb bud tissue has been fine-tuned by evolution of the system's parameters. The 2GL model correspondingly predicts, in principle, the full diversity of limb skeletal architectures across both sides of the fin-limb transition.

We know from videomicrography of living micromass structures that the protocondensations produced by the core network are not inherently skeleton-like, i.e., immobile, or stiff. In fact, they are liquid-like foci, containing cells in more rapid relative motion than those surrounding them, despite the elevated concentration of Gal-1A at those sites (Glimm et al., 2021). For such foci eventually to become arranged into the primordia of a skeleton, that is, masses and extended rods of rigid tissue,

it was necessary that the molecule that first induces the cells to congregate, i.e., Gal-1A, not be produced in an intermittent fashion. If it were, the sites of congregation (i.e., protocondensations) would be transient and discontinuous.

By mathematical analysis, we have determined that in contrast to many Turing-type and other reaction-diffusion systems that have been studied computationally, the spatially independent core network of the 2GL system is not capable of exhibiting oscillatory behavior. Analytically, this can be deduced from a Lyapunov function of the system's variables and parameters that elucidates the behavior depicted in Fig. 5. However, an oscillation-resistant system for producing the initiator of protocondensation (i.e., Gal-1A) is a natural core mechanism for skeletal development. Its incorporation into a more elaborate, spatially dependent network (via diffusion and adhesion-based flux) made it capable of forming repeated structures independently of oscillation (Fig. 3). This enabled the generation of a reliably patterned skeleton of discrete, cohesive elements instead of (as would result from the core mechanism on its own) a collection of mesenchymal droplets of indeterminate size and spacing. We can speculate that an ancient galectin-based cell state-switching mechanism may have evolved to disable any oscillatory potential as the galectin-rich sites also became foci of haptotaxis.

The limb skeletogenesis network does contain a temporally oscillating component, Hes1, which interacts with the wave-forming ones. If the oscillations of this transcriptional coregulator are suppressed, the arrangement of cartilage elements, and the condensations that prefigure them, become less regular (Fig. 5). We hypothesized that the concentration of Hes1 (and thus its phase, since it oscillates) controls the flux of cells up the gradient of Gal-1A and built this into the spatially dependent 2GL model. While this expanded model was based on indirect evidence, it was able to predict the elevation of both Gal-1A and Gal-8 production that accompanies the suppression of Hes1 oscillations (Bhat et al., 2019). Furthermore, simulations (summarized above) accounted for the loss of regularity in the patterning process shown in Fig. 3. This only occurred, however, when the model cells expressed Hes1 in the 'oscillatory synchronous' or 'nonoscillatory uniform' modes (Fig. 6, a, c).

The implication was that when the concentration of Hes1 (a key factor of cell responsivity) was the same across the field of cells (alternatively, the morphogenetically active zone at the tip of the limb bud at successive stages of development, or the micromass cultures constructed with autopodial cells), the standing wave-generating 2GL mechanism acts on a uniformly responsive medium, achieving the same effect for the same signal strengths throughout the domain. In contrast, when the Hes1 status is uneven across the field (as it is in the 'oscillatory asynchronous' and 'nonoscillatory random' modes (Fig. 6 b, d)), the point-to-point response across the cell fields would be uneven or noisy.

It would be nearly impossible for the embryo to arrange for the Hes1 status to be identical in every cell across the respective morphogenetic fields by employing the 'nonoscillatory uniform' mode (Fig. 6c). But it is a straightforward matter, a physical side-effect, for cells oscillating in Hes1 production to come into spontaneous synchrony (Fig. 6a). Even though the Hes1 concentration would change periodically, at each point in time it would be the same from cell to cell, and the 2GL mechanism would elicit smooth responses across the spatial domain. Paradoxically, then, the oscillatory process would be acting not in its capacity to effect temporal change but, by effecting spatial uniformity, to refine the action of a standing wave-forming process. A similar effect occurs in somitogenesis, where synchronization of Hes1 oscillations produces coherently responding tissues (Giudicelli et al., 2007). But there, since the organizing signal is a moving front which acts on the tissue at a specific phase of Hes1 cycle, the oscillatory process leaves its mark on the tissue as a periodic array of segments. In the limb, in contrast, the periodic spatial periodicity results from a separate process, and the Hes1 oscillation leaves no morphological trace, except through perturbation.

Acknowledgement

S.A.N., R.B. and T.G. together framed this conceptual review. The experiments presented, from our earlier and forthcoming publications, were performed by R.B., and the simulations, similarly from our earlier work, were performed by T.G., and in the case of Fig. 3, with the collaboration of Dr. Jianying Zhang. The authors are grateful to Dr. Luigia Santella for her suggestion that we write about this subject for *BioSystems*. R.B. is supported by Wellcome Trust/DBT India Alliance Fellowship/Grant [IA/I/17/2/503312] and the Department of Biotechnology, India (BT/909 PR26526/GET/119/92/2017). The authors declare that they have no competing interests.

References

Armstrong, N.J., Painter, K.J., Sherratt, J.A., 2006. A continuum approach to modelling cell-cell adhesion. J. Theor. Biol. 243, 98–113.
Aulehla, A., Pourquie, O., 2006. On periodicity and directionality of somitogenesis. Anat. Embryol. 211 (Suppl. 7), 3–8.
Badugu, A., Kraemer, C., Germann, P., Menshykau, D., Iber, D., 2012. Digit patterning during limb development as a result of the BMP-receptor interaction. Sci. Rep. 2, 991.
Barna, M., Niswander, L., 2007. Visualization of cartilage formation: insight into cellular properties of skeletal progenitors and chondrodysplasia syndromes. Dev. Cell 12, 931–941.
Bhat, R., Chakraborty, M., Glimm, T., Stewart, T.A., Newman, S.A., 2016. Deep phylogenomics of a tandem-repeat galectin regulating appendicular skeletal pattern formation. BMC Evol. Biol. 16, 162.
Bhat, R., Glimm, T., Linde-Medina, M., Cui, C., Newman, S.A., 2019. Synchronization of Hes1 oscillations coordinates and refines condensation formation and patterning of the avian limb skeleton. Mech. Dev. 156, 41–54.
Bhat, R., Lerea, K.M., Peng, H., Kaltner, H., Gabius, H.J., Newman, S.A., 2011. A regulatory network of two galectins mediates the earliest steps of avian limb skeletal morphogenesis. BMC Dev. Biol. 11, 6.
Chen, C., Liu, S., Shi, X.Q., Chate, H., Wu, Y., 2017. Weak synchronization and large-scale collective oscillation in dense bacterial suspensions. Nature 542, 210–214.
Christley, S., Alber, M.S., Newman, S.A., 2007. Patterns of mesenchymal condensation in a multiscale, discrete stochastic model. PLoS Comput. Biol. 3 (e76), 0743-0753.
Clark, E., 2017. Dynamic patterning by the Drosophila pair-rule network reconciles long-germ and short-germ segmentation. PLoS Biol. 15, e2002439.
Clark, E., Peel, A.D., Akam, M., 2019. Arthropod segmentation. Development 146, dev170480.
Cooke, J., Zeeman, E.C., 1976. A clock and wavefront model for control of the number of repeated structures during animal morphogenesis. J. Theor. Biol. 58, 455–476.
Cooper, K.L., 2015. Self-organization in the limb: a Turing mechanism for digit development. Curr. Opin. Genet. Dev. 32, 92–97.
Cotterell, J., Robert-Moreno, A., Sharpe, J., 2015. A local, self-organizing reaction-diffusion model can explain somite patterning in embryos. Cell Syst. 1, 257–269.
Cross, M.C., Hohenberg, P., 1993. Pattern formation outside of equilibrium. Rev. Mod. Phys. 65, 851–1112.
El-Sherif, E., Averof, M., Brown, S.J., 2012. A segmentation clock operating in blastoderm and germband stages of Tribolium development. Development 139, 4341–4346.
Franssen, R.A., Marks, S., Wake, D., Shubin, N., 2005. Limb chondrogenesis of the seepage salamander, Desmognathus aeneus (Amphibia: plethodontidae). J. Morphol. 265, 87–101.
Frenz, D.A., Jaikaria, N.S., Newman, S.A., 1989. The mechanism of precartilage mesenchymal condensation: a major role for interaction of the cell surface with the amino-terminal heparin-binding domain of fibronectin. Dev. Biol. 136, 97–103.
Garcia-Ojalvo, J., Elowitz, M.B., Strogatz, S.H., 2004. Modeling a synthetic multicellular clock: repressilators coupled by quorum sensing. Proc. Natl. Acad. Sci. U. S. A. 101, 10955–10960.
Gilbert, S.F., Sarkar, S., 2000. Embracing complexity: organicism for the 21st century. Dev. Dynam. 219, 1–9.
Giudicelli, F., Özbudak, E.M., Wright, G.J., Lewis, J., 2007. Setting the tempo in development: an investigation of the zebrafish somite clock mechanism. PLoS Biol. 5, e150.
Glimm, T., Bhat, R., Newman, S.A., 2014. Modeling the morphodynamic galectin patterning network of the developing avian limb skeleton. J. Theor. Biol. 346, 86–108.
Glimm, T., Kaźmierczak, B., Cui, C., Newman, S.A., Bhat, R., 2021. Modeling the bistable transition between cell phenotypes during limb precartilage condensation, 2021 bioRxiv 2003, 2015, 435301.
Glimm, T., Zhang, J., 2020. Numerical approach to a nonlocal advection-reaction-diffusion model of cartilage pattern formation. Math. Comput. Appl. 25, 36.
Hentschel, H.G., Glimm, T., Glazier, J.A., Newman, S.A., 2004. Dynamical mechanisms for skeletal pattern formation in the vertebrate limb. Proc. R. Soc. Lond. B Biol. Sci. 271, 1713–1722.
Hinchliffe, J.R., Johnson, D.R., 1980. The Development of the Vertebrate Limb. Oxford University Press, Oxford.
Hubaud, A., Pourquie, O., 2014. Signalling dynamics in vertebrate segmentation. Nat. Rev. Mol. Cell Biol. 15, 709–721.

Hubaud, A., Regev, I., Mahadevan, L., Pourquie, O., 2017. Excitable dynamics and yap-dependent mechanical cues drive the segmentation clock. Cell 171, 668–682 e611.
Jahnke, W., Henze, C., Winfree, A.T., 1988. Chemical vortex dynamics in three-dimensional excitable media. Nature 336, 662–665.
Just, W., Bose, M., Bose, S., Engel, H., Schöll, E., 2001. Spatiotemporal dynamics near a supercritical Turing-Hopf bifurcation in a two-dimensional reaction-diffusion system. Phys. Rev. E - Stat. Nonlinear Soft Matter Phys. 64, 026219.
Kaltner, H., Gabius, H.J., 2012. A toolbox of lectins for translating the sugar code: the galectin network in phylogenesis and tumors. Histol. Histopathol. 27, 397–416.
Kiskowski, M.A., Alber, M.S., Thomas, G.L., Glazier, J.A., Bronstein, N.B., Pu, J., Newman, S.A., 2004. Interplay between activator-inhibitor coupling and cell-matrix adhesion in a cellular automaton model for chondrogenic patterning. Dev. Biol. 271, 372–387.
Kondo, S., Miura, T., 2010. Reaction-diffusion model as a framework for understanding biological pattern formation. Science 329, 1616–1620.
Lange, Axel, Nemeschkal, H.L., Müller, G.B., 2018. A threshold model for polydactyly. Prog. Biophys. Mol. Biol. 137, 1–11.
Levin, M., 2012. Morphogenetic fields in embryogenesis, regeneration, and cancer: non-local control of complex patterning. Biosystems 109, 243–261.
McQueen, C., Towers, M., 2020. Establishing the pattern of the vertebrate limb. Development 147.
Meinhardt, H., Gierer, A., 2000. Pattern formation by local self-activation and lateral inhibition. Bioessays 22, 753–760.
Motani, R., 1999. On the evolution and homologies of ichthyopterygian forefins. J. Vertebr. Paleontol. 19, 28–41.
Newman, S.A., 1993. Is segmentation generic? Bioessays 15, 277–283.
Newman, S.A., Frisch, H.L., 1979. Dynamics of skeletal pattern formation in developing chick limb. Science 205, 662–668.
Newman, S.A., Glimm, T., Bhat, R., 2018. The vertebrate limb: an evolving complex of self-organizing systems. Prog. Biophys. Mol. Biol. 137, 12–24.
Ochi, S., Imaizuma, Y., Shimojo, H., Miyachi, H., Kageyama, R., 2020. Oscillatory expression of Hes1 regulates cell proliferation and neuronal differentiation in the embryonic brain. Development 147, dev182204.
Özbudak, E.M., Lewis, J., 2008. Notch signalling synchronizes the zebrafish segmentation clock but is not needed to create somite boundaries. PLoS Genet. 4, e15.
Palmeirim, I., Henrique, D., Ish-Horowicz, D., Pourquié, O., 1997. Avian hairy gene expression identifies a molecular clock linked to vertebrate segmentation and somitogenesis. Cell 91, 639–648.
Raspopovic, J., Marcon, L., Russo, L., Sharpe, J., 2014. Modeling digits. Digit patterning is controlled by a Bmp-Sox9-Wnt Turing network modulated by morphogen gradients. Science 345, 566–570.
Rida, P.C., Le Minh, N., Jiang, Y.J., 2004. A Notch feeling of somite segmentation and beyond. Dev. Biol. 265, 2–22.
Roselló-Díez, A., Arques, C.G., Delgado, I., Giovinazzo, G., Torres, M., 2014. Diffusible signals and epigenetic timing cooperate in late proximo-distal limb patterning. Development 141, 1534–1543.
Salazar-Ciudad, I., Jernvall, J., Newman, S.A., 2003. Mechanisms of pattern formation in development and evolution. Development 130, 2027–2037.
Salazar-Ciudad, I., Solé, R.V., Newman, S.A., 2001. Phenotypic and dynamical transitions in model genetic networks. II. Application to the evolution of segmentation mechanisms. Evol. Dev. 3, 95–103.
Seymour, P., et al., 2020. Jag1 modulates an oscillatory Dll1-Notch-Hes1 signaling module to coordinate growth and fate of pancreatic progenitors. Dev. Cell 52, 731–747.
Sheth, R., Marcon, L., Bastida, M.F., Junco, M., Quintana, L., Dahn, R., Kmita, M., Sharpe, J., Ros, M.A., 2012. Hox genes regulate digit patterning by controlling the wavelength of a Turing-type mechanism. Science 338, 1476–1480.
Stern, C.D., Piatkowska, A.M., 2015. Multiple roles of timing in somite formation. Semin. Cell Dev. Biol. 42, 134–139.
Strogatz, S.H., 2003. Sync: the Emerging Science of Spontaneous Order, first ed. Theia, New York.
Turing, A.M., 1952. The chemical basis of morphogenesis. Phil. Trans. Roy. Soc. Lond. B 237, 37–72.
Vasiliauskas, D., Laufer, E., Stern, C.D., 2003. A role for hairy1 in regulating chick limb bud growth. Dev. Biol. 262, 94–106.
Verd, B., Clark, E., Wotton, K.R., Janssens, H., Jimenez-Guri, E., Crombach, A., Jaeger, J., 2018. A damped oscillator imposes temporal order on posterior gap gene expression in Drosophila. PLoS Biol. 16, e2003174.
West-Eberhard, M.J., 2003. Developmental Plasticity and Evolution. Oxford University Press, Oxford; New York.
Young, N.M., Winslow, B., Takkellapati, S., Kavanagh, K., 2015. Shared rules of development predict patterns of evolution in vertebrate segmentation. Nat. Commun. 6, 6690.
Zhu, J., Zhang, Y.T., Alber, M.S., Newman, S.A., 2010. Bare bones pattern formation: a core regulatory network in varying geometries reproduces major features of vertebrate limb development and evolution. PloS One 5, e10892.